Post-coordination functionalisation of pyrazolyl-based ligands as a route to polynuclear complexes based on an inert $Ru^{II}N_6$ core

Qiao-Hua Wei, Stephen P. Argent, Harry Adams and Michael D. Ward*

Received (in Durham, UK) 6th June 2007, Accepted 30th August 2007
First published as an Advance Article on the web 10th September 2007
DOI: 10.1039/b708572a

The simple mononuclear complex $[Ru(H_2bpp)_2][PF_6]_2$ [H_2bpp = 2,6-bis(pyrazol-3-yl)pyridine] contains four coordinated pyrazolyl ligands which each have a reactive NH site at the position adjacent to the coordinated N atom. Alkylation of these with either 2-[1-{4-(bromomethyl)benzyl}-1*H*-pyrazol-3-yl]pyridine or 4′-[(4-bromomethyl)phenyl]terpyridine allows attachment of four additional chelating groups, either bidentate pyrazolyl–pyridine and terdentate terpyridyl units, respectively, which are pendant from the central kinetically inert $Ru^{II}N_6$ complex core. These functionalised mononuclear complexes $[Ru(L^1)_2][PF_6]_2$ (with four pendant pyrazolyl–pyridine bidentate sites) and $[Ru(L^2)_2][PF_6]_2$ (with four pendant terpyridyl sites) can be used as the starting point for polynuclear assemblies by attachment of additional labile metal ions as the secondary sites. As examples of this we prepared and structurally characterised the trinuclear complex $[RuAg_2(L^1)_2][ClO_4]_4$, an unusual example of a polynuclear helicate containing a kinetically inert metal centre, and the pentanuclear complex $[RuCu_4(MeCN)_5(H_2O)_{1.5}(L^2)_2](SbF_6)_6(BF_4)_4$ in which each of the pendant terpyridyl sites of the $[Ru(L^2)_2]^{2+}$ core is coordinated to a Cu(II) ion.

Introduction

For practitioners of modern coordination chemistry it is a common requirement to be able to synthesise polynuclear complexes in which different metal ions occupy different sites of a multinucleating ligand which contains different binding domains. The problems under investigation can be highly varied (small molecule activation or catalysis by cooperative binding at a polynuclear site;[1] photoinduced energy or electron transfer from one metal complex fragment to another;[2] electrochemical interactions across a conjugated bridging ligand[3]) but the basic synthetic problem is the same in every case. There are two general methods which may be employed. Firstly, if kinetically labile metal ions are used, a multi-topic ligand may be treated with a mixture of metal ions and a single product results in which each ion has sought out the binding domain which given the most thermodynamically stable product. This is illustrated by our recent one-pot preparation of the heteronuclear helicate $[FeAg_2(L^1)_2]^{4+}$, in which the propensity of Fe(II) for six-fold coordination and of Ag(I) for four-fold coordination led to these ions occupying the central and peripheral sites, respectively of the double helical structure.[4] Alternatively, if kinetically inert metal ions are used, a stepwise 'complexes as ligands' approach has to be employed in which the binding sites of a multi-topic ligand are occupied sequentially.[2,3,5] It can be difficult to put a single kinetically inert ion at one site of a multi-topic ligand, because mixtures of mononuclear and polynuclear complexes inevitably result which require careful separation.

Department of Chemistry, University of Sheffield, Sheffield, UK S3 7HF. E-mail: m.d.ward@sheffield.ac.uk

Consequently, a better method is to make a coordinatively saturated mononuclear complex with a reactive peripheral site. Attachment of a second ligand fragment to this complex core, or even attachment of an entire additional complex fragment, provides an efficient stepwise method for assembly of heteropolynuclear complexes. This method is illustrated by work from the groups of Constable[6] and Tor.[7] Constable has shown how complexes of functionalised 2,2′:6′,2″-terpyridines can be used as building blocks to make polynuclear dendrimer-like complexes of Ru(II) and Os(II), by reaction together of $\{M(terpy)_2\}^{2+}$ species with complementary reactive functional groups (*e.g.* hydroxyl, halogen) at their peripheries.[6] Tor has shown how two complexes, one containing a 5-bromophenanthroline ligand and the other containing an ethynylphenanthroline ligand, can be coupled using conventional organic synthetic methodology to give a heterodinuclear complex containing an alkyne-linked bis-phenanthroline ligand.[7]

In this paper we illustrate a new variant on this theme, in which alkylation of the pyrazole rings of a coordinated terdentate ligand allows additional ligand sites to be added around the periphery of a kinetically inert Ru(II) core. The resulting mononuclear Ru(II) complexes then contain four peripheral bidentate or tridentate sites, and these species can be used as the basis for assembly of polynuclear complexes which would not be accessible from the pre-formed complete ligands.

Results and discussion

Preparation of mononuclear complexes with pendant binding sites

For this work we employed the terdentate ligand 2,6-bis(pyrazol-3-yl)pyridine (H_2bpp) which coordinates as a

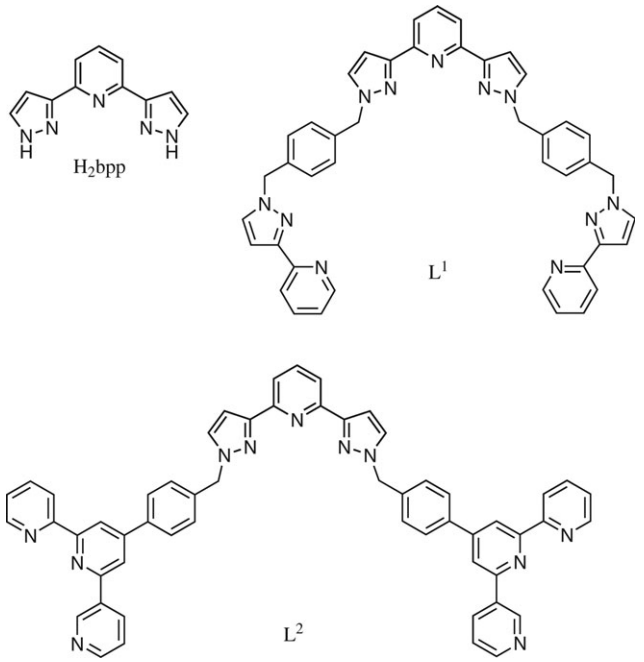

Scheme 1 Structural formulae of the ligands described in this paper.

simple tridentate chelate, but which has reactive pyrazolyl NH groups that can be functionalised further (Scheme 1). We reported the synthesis of this ligand a while ago and described some of its lanthanide(III) complexes.[8] Reaction of commercial ruthenium(III) chloride with two equivalents of H_2bpp in ethylene glycol at reflux afforded, after chromatographic purification and anion metathesis with ammonium hexafluorophosphate, the mononuclear complex $[Ru(H_2bpp)_2][PF_6]_2$ in good yield. The crystal structure of the complex (Fig. 1, Table 1) reveals a conventional slightly distorted octahedral coordination geometry. The Ru–N(pyridyl) bond distances to the central rings of the ligands are slightly shorter (average 2.019 Å) than the Ru–N(pyrazolyl) bond distances, which average 2.072 Å; this follows the normal pattern for complexes of terpyridine in which the central pyridyl ring generally has the shortest metal–ligand bond for steric

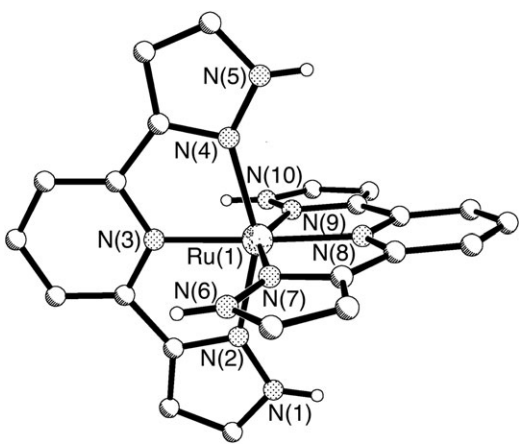

Fig. 1 Structure of the complex cation of $[Ru(H_2bpp)_2][PF_6]_2 \cdot 2Et_2O \cdot 2MeCN$ (H atoms, except for pyrazolyl N–H atoms, removed for clarity).

Table 1 Selected bond distances (Å) and angles (°) for $[Ru(H_2bpp)_2][PF_6]_2 \cdot 2Et_2O \cdot 2MeCN$

Ru(1)–N(8)	2.016(3)	Ru(1)–N(7)	2.068(3)
Ru(1)–N(3)	2.021(3)	Ru(1)–N(2)	2.076(3)
Ru(1)–N(9)	2.066(3)	Ru(1)–N(4)	2.076(3)
N(8)–Ru(1)–N(3)	177.74(13)	N(9)–Ru(1)–N(2)	90.60(13)
N(8)–Ru(1)–N(9)	77.19(13)	N(7)–Ru(1)–N(2)	93.77(13)
N(3)–Ru(1)–N(9)	102.77(13)	N(8)–Ru(1)–N(4)	100.80(13)
N(8)–Ru(1)–N(7)	77.13(13)	N(3)–Ru(1)–N(4)	76.94(14)
N(3)–Ru(1)–N(7)	102.99(13)	N(9)–Ru(1)–N(4)	93.98(13)
N(9)–Ru(1)–N(7)	154.20(14)	N(7)–Ru(1)–N(4)	93.15(13)
N(8)–Ru(1)–N(2)	105.19(13)	N(2)–Ru(1)–N(4)	153.98(14)
N(3)–Ru(1)–N(2)	77.07(13)		

reasons.[9] The N(pyrazolyl)–Ru–N(pyrazolyl) bite angles are both 154°, and the two terdentate ligands are essentially mutually perpendicular.

The UV/Vis spectroscopic and redox properties of $[Ru(H_2bpp)_2][PF_6]_2$ can be understood with reference to the known electronic properties of pyrazole groups as ligands compared to pyridyl groups, *viz*. pyrazolyl ligands are poorer σ-donors than pyridyl ligands (*cf*. the pK_a values for protonation of 5.2 for pyridine and 2.6 for pyrazole), and are also much poorer π-acceptors with high-energy π* orbitals compared to polypyridines.[10] The latter effect dominates such that compared to $[Ru(terpy)_2]^{2+}$,[11] for example, the metal centre of $[Ru(H_2bpp)_2][PF_6]_2$ is more electron-rich and accordingly has a less positive Ru(II)/Ru(III) redox potential (+0.54 V *vs*. Fc/Fc^+, *cf*. +0.89 V for $[Ru(terpy)_2]^{2+}$). This effect is formalised in Lever's electrochemical parameters for the different ligand types in Ru(II)/Ru(III) complexes.[12] The poor π-accepting ability of the H_2bpp ligands compared to terpy is reflected in a higher π* energy, resulting in a blue-shifted ^{1}MLCT absorption compared to $[Ru(terpy)_2]^{2+}$ (418 nm *vs*. 470 nm,[11] respectively).

From the structural point of view of further functionalisation at the pyrazolyl NH sites, the geometry of the complex is ideal with the two pyrazolyl N–H vectors of one H_2bpp ligand being essentially parallel to the plane of the other ligand between them. Thus, any substituents attached at these sites will not diverge too much from the complex core, and will not interfere sterically with the other ligand. This situation may be contrasted with the situation when a $[Ru(terpy)_2]^{2+}$ core is used as the basis for further functionalisation (Scheme 2). In this case, the pinching of the terpy ligand on coordination to Ru(II) means that substituents at the C^6 and $C^{6''}$ positions converge on the other ligand and interfere with it sterically, resulting in the complexes becoming particularly labile;[13] the C^5 and $C^{5''}$ positions however are still divergent, and are notably difficult positions at which to introduce substituents.[14] Thus $[Ru(H_2bpp)_2][PF_6]_2$ provides a geometrically ideal scaffold for synthetically facile further functionalisation of an octahedral metal complex core.

Reaction of $[Ru(H_2bpp)_2][PF_6]_2$ with >4 equivalents of 2-[1-{4-(bromomethyl)benzyl}-1*H*-pyrazol-3-yl]pyridine to afford $[Ru(L^1)_2][PF_6]_2$ (Scheme 3) was investigated under a variety of conditions. In the end the best conditions were found to be MeCN–CH_2Cl_2 (3 : 1) as solvent at 80 °C, using NaH as base to deprotonate the pyrazole groups of $[Ru(H_2bpp)_2][PF_6]_2$ (use of alternative bases such as Et_3N or

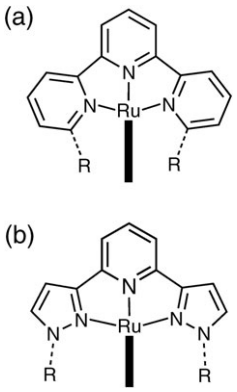

Scheme 2 Illustration of the different extents to which ligand substituents (R) converge on, and sterically interfere with, the alternate ligand using (a) terpyridine and (b) H_2bpp, coordinated to a six-coordinate Ru(II) centre. The second ligand is shown edge-on as a thick black bar.

Bu_4NOH was much less successful), and using a catalytic amount of Bu_4NI to speed up the nucleophilic substitution at the CH_2Br sites. Under these conditions we could effect the tetraalkylation of $[Ru(H_2bpp)_2][PF_6]_2$ to give $[Ru(L^1)_2][PF_6]_2$ in 26% yield, as confirmed by the ESI mass spectrum and ^1H NMR spectrum (see Experimental section). The ligand L^1 is the same one that we described earlier and used to form polynuclear helicates;[4] however, it is clear that reaction of pre-formed L^1 with a source of Ru(II) would be very unlikely to have given significant quantities of $[Ru(L^1)_2][PF_6]_2$ but would have generated a complicated mixture of products.

A small amount of $[Ru(L^1)_2][PF_6]_2$ was converted to the nitrate salt to grow X-ray quality crystals. The structure of $[Ru(L^1)_2](NO_3)_2$ (Fig. 2, Table 2) has some interesting features. The complex crystallises in the space group $I\bar{4}$ such that only one quarter of the cation is unique. The phenyl ring of each pendant arm is almost perpendicular to the pyrazolyl ring from which it is pendant (angle between mean planes of 88.5°), and is involved in an aromatic π-stacking interaction with a coordinated pyrazolyl ring from the alternate ligand; the stacked phenyl and pyrazolyl rings are *ca.* 3.5 Å apart and nearly parallel (angle of 9.3° between their mean planes). This stacking interaction is facilitated by the ideal geometry of the complex core as described above, which results in each pendant phenyl group neither diverging from nor converging with

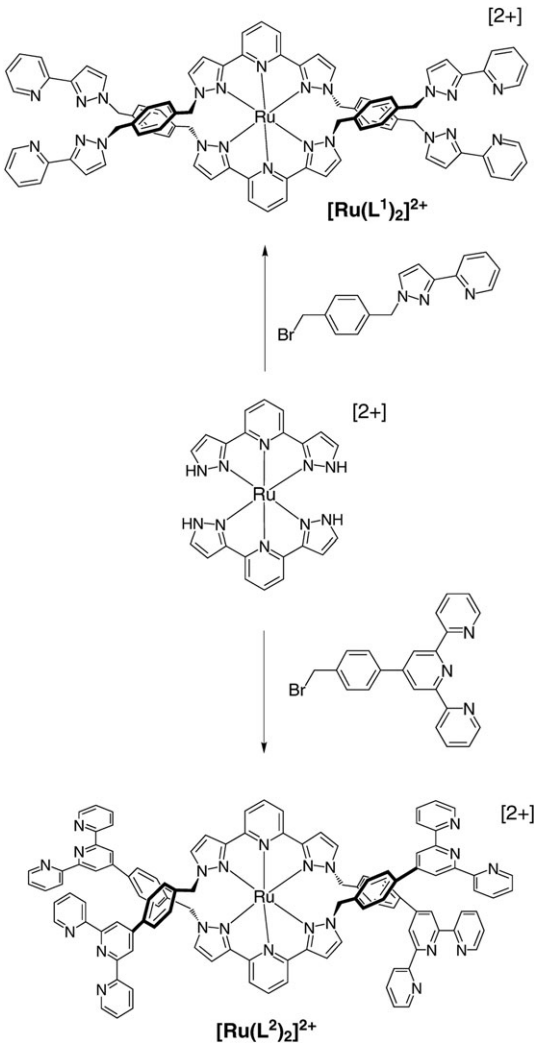

Scheme 3 Syntheses and structural formulae of the complexes $[Ru(L^1)_2]^{2+}$ and $[Ru(L^2)_2]^{2+}$, bearing four pendant bipyridyl or terpyridyl sites, respectively.

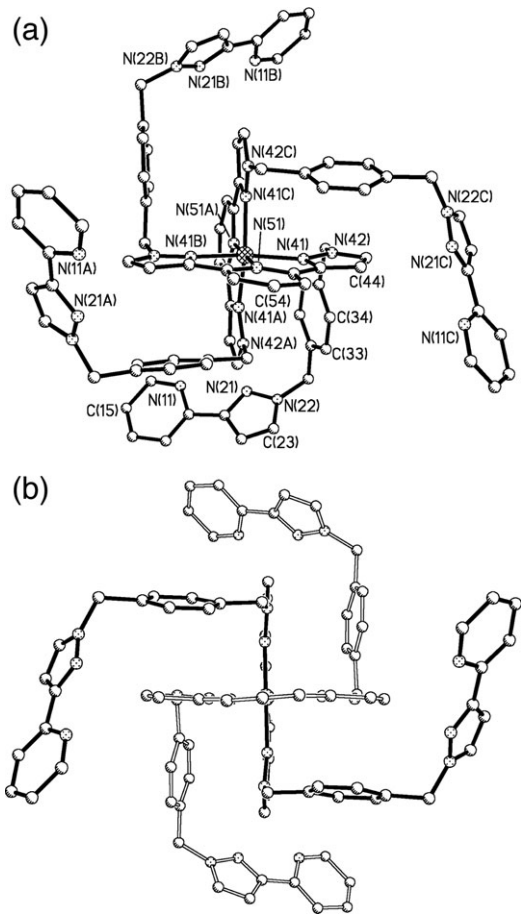

Fig. 2 Two views of the complex cation of $[Ru(L^1)_2](NO_3)_2$. (a) A view showing the atom labeling scheme. The symmetry operations invoked by the additional labels A, B, C are as follows: A $(-1 + y, 1 - x, 2 - z)$, B $(-x, 2 - y, z)$, C $(1 - y, 1 + x, 2 - z)$. (b) A view down the $\bar{4}$ axis with the two ligands shaded separately for clarity.

Table 2 Selected bond distances (Å) and angles (°) for $[Ru(L^1)_2](NO_3)_2 \cdot 4H_2O$

Ru(1)–N(51)	2.034(2)
Ru(1)–N(41)	2.0894(19)
N(51A)–Ru(1)–N(51)	180.0
N(51A)–Ru(1)–N(41)	103.46(6)
N(51)–Ru(1)–N(41)	76.54(6)
N(41B)–Ru(1)–N(41)	153.08(11)
N(41)–Ru(1)–N(41A)	93.11(3)

Symmetry transformations used to generate equivalent atoms. A: $y-1$, $-x+1$, $-z+2$. B: $-x$, $-y+2$, z.

Table 3 Selected bond distances (Å) and angles (°) for $[Ru(L^2)_2][PF_6]_2 \cdot C_6H_6$

Ru(1)–N(61)	2.026(3)	Ru(1)–N(71)	2.102(3)
Ru(1)–N(51)	2.094(3)		
N(61)–Ru(1)–N(61A)	175.67(15)	N(51)–Ru(1)–N(71A)	99.47(11)
N(61)–Ru(1)–N(51A)	106.43(11)	N(61)–Ru(1)–N(71)	77.00(11)
N(61)–Ru(1)–N(51)	76.84(11)	N(61A)–Ru(1)–N(71)	99.80(11)
N(51A)–Ru(1)–N(51)	85.80(15)	N(51)–Ru(1)–N(71)	153.75(11)
N(61)–Ru(1)–N(71A)	99.80(11)	N(71A)–Ru(1)–N(71)	87.15(17)

Symmetry transformations used to generate equivalent atoms. A: $-x+1/2$, $-y$, z.

the other ligand, but lying parallel to it at an appropriate distance for π-stacking.

Under similar conditions, we could prepare $[Ru(L^2)_2][PF_6]_2$ by alkylation of the four pyrazolyl rings of $[Ru(H_2bpp)_2][PF_6]_2$ with an excess of 4′-[(4-bromomethyl)phenyl]terpyridine (Scheme 3) in 49% yield. Again, ESI mass spectrometry and ^{1}H NMR spectroscopy confirmed the formulation of the product with four pendant terpyridyl groups. The crystal structure of $[Ru(L^2)_2][PF_6]_2 \cdot C_6H_6$ is shown in Fig. 3 with selected parameters in Table 3. In this case two of the four pendant groups have their phenyl groups [C(41)–C(46) and its symmetry equivalent] involved in aromatic stacking interactions with a coordinated pyrazolyl ring from the alternate ligand [N(71)–C(75) and its symmetry equivalent], and the two ligands are entwined around one another in a pseudo-helical manner.

$[Ru(L^1)_2][PF_6]_2$ and $[Ru(L^2)_2][PF_6]_2$ have very similar redox potentials (+0.75 and +0.77 V *vs.* Fc/Fc^+, respectively) and identical ^{1}MLCT absorption maxima (402 nm). The positive shift of the Ru(II)/Ru(III) redox couple of *ca.* 200 mV on alkylation of the four pyrazole rings of $[Ru(H_2bpp)_2][PF_6]_2$ implies a decrease in electron density at the metal centre compared to $[Ru(H_2bpp)_2][PF_6]_2$ because L^1 and L^2 are poorer σ-donors or better π-acceptors (or a combination of both). If the alkylated ligands L^1 and L^2 were better π-acceptors than H_2bpp, the ^{1}MLCT absorption maximum would be expected to be red-shifted compared to $[Ru(H_2bpp)_2][PF_6]_2$ as the ligand-based π* energy is reduced. In fact the converse is true, implying that the main effect of alkylation of the pyrazole groups is to make L^1 and L^2 poorer σ-donors, because the pyrazole rings have less $pz^- \cdots H^+$ character when the potentially acidic protons are replaced by alkyl groups.

Polynuclear complexes

Since $[Ru(L^1)_2][PF_6]_2$ has pendant bidentate chelating units, reaction with an excess of $AgClO_4$ was carried out to see if four-coordinate (bis-bidentate) Ag(I) centres could form as part of a polynuclear assembly. Assuming that two of the four pendant bidentate units coordinate to each Ag(I) centre, this could afford one of two types of structure. If the two pendant pyrazolyl–pyridine units from the *same* ligand coordinated to each Ag(I) ion, the result would be a catenated structure in which two metallamacrocycles [Ag/L^1 loops] are connected by coordination of each of their terdentate sites to the central Ru(II).[15] Alternatively, if the two pyrazolyl–pyridine units which bind to each Ag(I) ion come from *different* ligands, the result will be a complexes in which each ligand spans all three metal ions, as we saw before in trinuclear double helicates with L^1.[4]

It is the second possibility which pertains here. The structure of $[RuAg_2(L^1)_2][ClO_4]_4$ (Fig. 4 and 5) is a trinuclear double helicate containing six-coordinate Ru(II) in the central cavity,

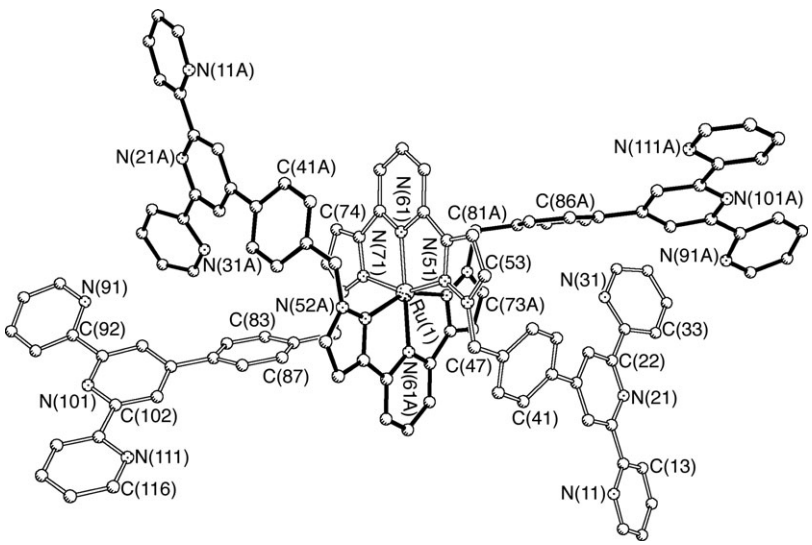

Fig. 3 Structure of the complex cation of $[Ru(L^2)_2][PF_6]_2 \cdot C_6H_6$, with the two ligands shaded separately for clarity.

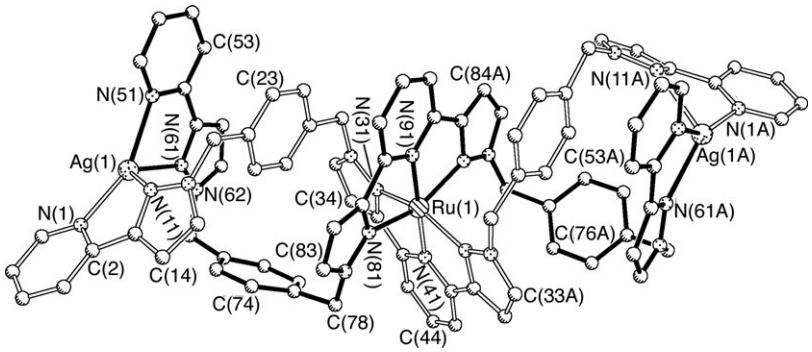

Fig. 4 Structure of the double helical complex cation of $[RuAg_2(L^1)_2][ClO_4]_4 \cdot H_2O \cdot 2dmf$, showing the atom labeling scheme.

and four-coordinate Ag(I) ions at the two peripheral sites in irregular four-coordinate geometries. The helical assembly is characterised by an extensive degree of stacking between the two intertwined ligands, which form a five-layer stack on one side of the complex involving terminal pyridyl/pyrazoles [coordinated to Ag(1)] of one ligand (denoted A), phenyl spacer groups of ligand B, and the central Ru(II)-bound pyridyl ring of ligand A. The Ru···Ag separation is 8.65 Å. This structure is generally similar to that of the $Fe^{II}Ag^{I}_2$ trinuclear helicate that we prepared recently in a one-pot reaction from labile Fe(II) and Ag(I) starting materials.[4] However the important difference is that this stepwise strategy has allowed the preparation of a helical scaffold based around a kinetically inert Ru(II) core, of which there are very few examples.[16] It is notable that in the ^{1}H NMR spectrum the two doublets arising from the central phenylene spacer groups are at low chemical shifts (6.47 and 5.64 ppm) which are indicative of the aromatic stacking involving these rings that is apparent in the crystal structure being retained in solution. However the presence of only two signals (an AX doublet-of-doublets) implies that all phenyl rings are in the same environment in solution, *i.e.* the complex has a more symmetric structure than that observed in the solid state. Given the lability of Ag(I) ions, and the distorted coordination environment about the Ag(I) ions with relatively long and weak Ag–N bonds (up to 2.5 Å, see Table 4), it is possible that the Ag(I) is undergoing a dissociation/reassociation equilibrium facilitated by the strong donor solvent which allows the phenylene groups to become equivalent in solution. The fact that the complex was only significantly soluble in dmso at the concentrations required for NMR spectroscopy unfortunately precluded low-temperature studies.

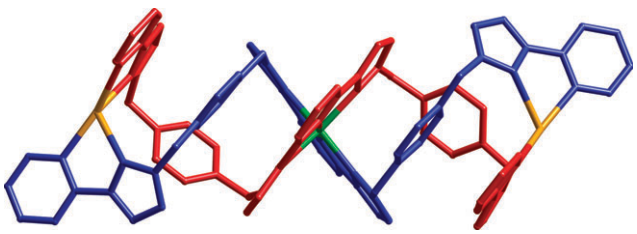

Fig. 5 Alternative view of the structure of the complex cation of $[RuAg_2(L^1)_2][ClO_4]_4 \cdot H_2O \cdot 2dmf$, with the ligands coloured separately for clarity.

With $[Ru(L^2)_2][PF_6]_2$ as the starting unit, there are likewise numerous possibilities for different architectures to form depending on how the pendant terpyridyl sites arrange themselves on coordination to the secondary metal ion. In principle trinuclear catenates or helicates could form, as with the previous example, if two of the terpyridyl sites can converge on the same metal centre. However this is not sterically likely given their divergent spatial arrangement. Simple attachment of one metal ion (plus ancillary ligands) at each terpyridyl site would give a pentanuclear species; coordination of two terpyridyl units from separate complexes to the same metal ion could easily result in infinite cross-linked chain structures with a fourfold-connected node at the Ru(II) centre.

Reaction of $[Ru(L^2)_2][PF_6]_2$ with $Zn(BF_4)_2$ in dmf, followed by precipitation of the product using $NaSbF_6$ and recrystallisation, afforded substantial and well-formed red crystals of a material whose elemental analysis indicated the formulation $[RuZn_2(L^2)_2](BF_4)_3(SbF_6)_3$, *i.e.* two Zn(II) ions per Ru(II) centre, implying that the Zn(II) ions are each coordinated by two terpyridyl sites. From inspection of Fig. 3 it is clear that it is not possible for two terpyridyl sites from the same Ru(II) complex unit to bind to the same Zn(II) ion, so the structure is likely to be a cross-linked network of some sort in which each Zn(II) ion is coordinated by pendant terpyridyls from two separate $[Ru(L^2)_2]^{2+}$ units. Frustratingly these crystals hardly scattered at all, even using synchrotron radiation, despite being large and well-formed, and it has not been possible to determine the structure of this network.

Table 4 Selected bond distances (Å) and angles (°) for $[RuAg_2(L^1)_2][ClO_4]_4 \cdot H_2O \cdot 2dmf$

Ru(1)–N(41)	2.005(7)	Ag(1)–N(1)	2.226(6)
Ru(1)–N(91)	2.035(7)	Ag(1)–N(61)	2.305(5)
Ru(1)–N(31)	2.090(5)	Ag(1)–N(51)	2.321(6)
Ru(1)–N(81)	2.109(4)	Ag(1)–N(11)	2.498(5)
N(41)–Ru(1)–N(91)	180.000(2)	N(1)–Ag(1)–N(61)	135.0(2)
N(41)–Ru(1)–N(31)	77.27(13)	N(1)–Ag(1)–N(51)	151.7(2)
N(91)–Ru(1)–N(31)	102.73(13)	N(61)–Ag(1)–N(51)	72.82(19)
N(31)–Ru(1)–N(31A)	154.5(3)	N(1)–Ag(1)–N(11)	71.4(2)
N(41)–Ru(1)–N(81)	102.89(13)	N(61)–Ag(1)–N(11)	121.29(16)
N(91)–Ru(1)–N(81)	77.11(13)	N(51)–Ag(1)–N(11)	99.66(18)
N(31)–Ru(1)–N(81)	98.50(16)		
N(31)–Ru(1)–N(81A)	87.17(16)		
N(81)–Ru(1)–N(81A)	154.2(3)		

Symmetry transformations used to generate equivalent atoms. A: $-x$, y, $-z + 1/2$.

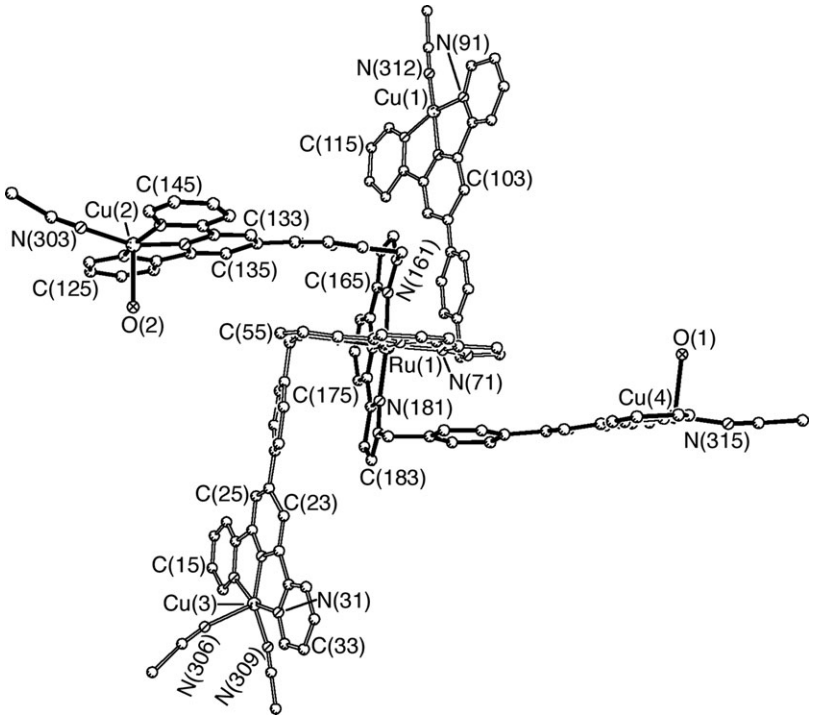

Fig. 6 Structure of the pentanuclear complex cation of $[RuCu_4(MeCN)_5(H_2O)_{1.5}(L^2)_2]$ $(SbF_6)_6(BF_4)_4 \cdot 5H_2O$, showing the atom labeling scheme.

We had more success by reaction of $[Ru(L^2)_2][PF_6]_2$ with four equivalents of $Cu(BF_4)_2$, followed by anion metathesis with $NaSbF_6$. Crystallisation of the crude product with $MeNO_2$/ether afforded in 25% yield green-brown crystals of the pentanuclear cluster $[RuCu_4(MeCN)_5(H_2O)_{1.5}$-$(L^2)_2](SbF_6)_6(BF_4)_4 \cdot 5H_2O$ in which each of the four pendant terpyridyl sites of the central $[Ru(L^2)_2]^{2+}$ core is occupied by a Cu(II) centre which is either four or five coordinate (from one terpyridyl ligand plus one or two monodentate solvent molecules). The crystal structure is shown in Fig. 6 and 7 and structural parameters are given in Table 5. The complex cation has approximate fourfold rotational symmetry, with each of the four Cu(II)–terpyridyl fragments being perpendicular to the plane of the pyrazolyl ring from which it is pendant. Each pendant phenyl ring is therefore parallel to and stacked with a pyrazolyl ring of the alternate ligand, with all four coordinated pyrazolyl rings of the Ru(II) core each interacting with one phenyl ring of a pendant arm. The coordination geometries around the Cu(II) centres are approximately square planar [Cu(1), with one MeCN ligand in addition to the terpy ligand]; square pyramidal [Cu(2), with equatorial MeCN and axial water ligands]; square pyramidal [Cu(3), with two MeCN ligands]; and a mixture of four- and five-coordinate [Cu(4), with an equatorial MeCN ligand and an axial water ligand which has a site occupancy of 0.5].

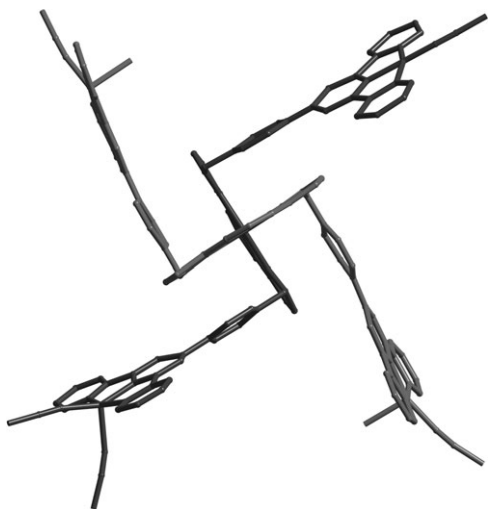

Fig. 7 Alternative view of the structure of the complex cation of $[RuCu_4(MeCN)_5(H_2O)_{1.5}(L^2)_2]$ $(SbF_6)_6(BF_4)_4 \cdot 5H_2O$, with the ligands coloured separately for clarity.

Conclusions

The functionalisation of the pyrazolyl groups of $[Ru(H_2bpp)_2][PF_6]_2$ with bipyridyl or terpyridyl fragments provides a kinetically inert Ru(II) complex core which can be used as the basis for preparation of polynuclear complexes and assemblies by addition of labile metal ions at the peripheral sites. This is a simple and effective route into multimetallic assemblies which would not be available by conventional self-assembly methods. Possibilities in the areas of photophysically active assemblies and coordination networks/crystal engineering are obvious and under investigation.

Experimental

General details

The following instrumentation was used for routine spectroscopic and electrochemical analyses: ^{1}H NMR spectra, Bruker AC-250, AMX2-400 or DRX-500 MHz spectrometers; EI and

Table 5 Selected bond distances (Å) and angles (°) for $[RuCu_4(MeCN)_5(H_2O)_{1.5}(L^2)_2]$ $(SbF_6)_6(BF_4)_4 \cdot 5H_2O$

Ru(1)–N(61)	2.026(17)	Cu(1)–N(101)	1.908(18)	Cu(2)–N(121)	2.00(2)	Cu(3)–N(306)	2.15(2)
Ru(1)–N(171)	2.035(15)	Cu(1)–N(91)	1.98(3)	Cu(2)–O(2)	2.27(4)	Cu(4)–N(211)	1.927(16)
Ru(1)–N(52)	2.064(16)	Cu(1)–N(111)	1.99(3)	Cu(3)–N(21)	1.934(18)	Cu(4)–N(315)	1.926(19)
Ru(1)–N(161)	2.085(15)	Cu(2)–N(131)	1.923(17)	Cu(3)–N(31)	1.98(2)	Cu(4)–N(201)	2.000(17)
Ru(1)–N(71)	2.097(16)	Cu(2)–N(303)	1.95(3)	Cu(3)–N(309)	1.99(2)	Cu(4)–N(221)	2.022(17)
Ru(1)–N(181)	2.100(17)	Cu(2)–N(141)	1.98(3)	Cu(3)–N(11)	2.00(2)	Cu(4)–O(1)	2.239(13)
Cu(1)–N(312)	1.74(3)						
N(61)–Ru(1)–N(171)	177.7(7)	N(161)–Ru(1)–N(181)	154.7(7)	N(141)–Cu(2)–N(121)	158.9(9)	N(309)–Cu(3)–N(306)	91.5(8)
N(61)–Ru(1)–N(52)	74.8(7)	N(71)–Ru(1)–N(181)	93.2(6)	N(131)–Cu(2)–O(2)	97.9(12)	N(11)–Cu(3)–N(306)	94.2(10)
N(171)–Ru(1)–N(52)	103.9(6)	N(312)–Cu(1)–N(101)	175.9(13)	N(303)–Cu(2)–O(2)	101.1(17)	N(211)–Cu(4)–N(315)	164.6(8)
N(61)–Ru(1)–N(161)	101.0(6)	N(312)–Cu(1)–N(91)	101.5(14)	N(141)–Cu(2)–O(2)	92.5(12)	N(211)–Cu(4)–N(201)	80.2(8)
N(171)–Ru(1)–N(161)	77.2(7)	N(101)–Cu(1)–N(91)	82.3(11)	N(121)–Cu(2)–O(2)	98.3(11)	N(315)–Cu(4)–N(201)	99.3(9)
N(52)–Ru(1)–N(161)	92.5(5)	N(312)–Cu(1)–N(111)	94.7(14)	N(21)–Cu(3)–N(31)	79.3(9)	N(211)–Cu(4)–N(221)	81.0(8)
N(61)–Ru(1)–N(71)	77.4(8)	N(101)–Cu(1)–N(111)	81.6(11)	N(21)–Cu(3)–N(309)	153.7(8)	N(315)–Cu(4)–N(221)	98.3(9)
N(171)–Ru(1)–N(71)	104.0(7)	N(91)–Cu(1)–N(111)	163.7(12)	N(31)–Cu(3)–N(309)	98.2(9)	N(201)–Cu(4)–N(221)	161.0(8)
N(52)–Ru(1)–N(71)	152.1(7)	N(131)–Cu(2)–N(303)	160.9(14)	N(21)–Cu(3)–N(11)	79.6(9)	N(211)–Cu(4)–O(1)	104.6(6)
N(161)–Ru(1)–N(71)	92.3(6)	N(131)–Cu(2)–N(141)	81.2(11)	N(31)–Cu(3)–N(11)	158.9(8)	N(315)–Cu(4)–O(1)	90.8(7)
N(61)–Ru(1)–N(181)	104.4(7)	N(303)–Cu(2)–N(141)	96.4(14)	N(309)–Cu(3)–N(11)	100.2(9)	N(201)–Cu(4)–O(1)	94.5(6)
N(171)–Ru(1)–N(181)	77.5(7)	N(131)–Cu(2)–N(121)	79.5(11)	N(21)–Cu(3)–N(306)	114.8(8)	N(221)–Cu(4)–O(1)	92.2(6)
N(52)–Ru(1)–N(181)	94.1(6)	N(303)–Cu(2)–N(121)	99.1(14)	N(31)–Cu(3)–N(306)	95.5(9)		

FAB mass spectra, a VG AutoSpec magnetic sector instrument; electrospray mass spectra, a Waters LCT instrument; IR spectra, a Perkin-Elmer Spectrum One instrument; UV/Vis spectra, a Cary-50 spectrometer. Cyclic voltammetric measurements were performed with an Ecochimie Autolab 100 potentiostat using a conventional three-electrode cell with a Pt wire working electrode; the base electrolyte was 0.1 M Bu_4NPF_6 and the solvent was MeCN.

All reactions were performed under an atmosphere of N_2 using standard Schlenk-line procedures. 2,6-bis(pyrazol-3-yl)-pyridine,[8] 2-[1-{4-(bromomethyl)benzyl}-1*H*-pyrazol-3-yl]pyridine,[4] and 4′-[(4-bromomethyl)phenyl]terpyridine[17] were prepared according to the published methods. Other organic reagents and metal salts were obtained from the usual commercial sources and used as received.

Syntheses

$[Ru(H_2bpp)_2][PF_6]_2$. A mixture of 2,6-bis(pyrazol-3-yl)pyridine (1.203 g, 5.7 mmol), $RuCl_3$ (0.472 g, 2.28 mmol) and ethylene glycol (14 cm^3) was heated to reflux with stirring for 26 h. After cooling the red mixture, excess aqueous NH_4PF_6 was added, and the mixture was refrigerated overnight to precipitate the complex which was filtered off and dried. The crude product was purified by column chromatography on silica using MeCN–water–saturated aqueous KNO_3 (40 : 4 : 1) as eluent. The first orange main band and the second red minor band were collected. The first orange fraction was then reduced in volume until the organic part of the solvent mixture was removed; the orange precipitate was filtered off, washed well with water to ensure complete removal of traces of KNO_3 and NH_4PF_6, and dried. Slow diffusion of diethyl ether vapour into a solution of the orange complex in acetonitrile in a few days afford the product $[Ru(H_2bpp)_2][PF_6]_2$ as orange–red crystals. Yield: 59%. Main IR peaks (KBr pellet, cm^{-1}): ν 560 (s), 767 (s), 838 (s, PF_6^-), 1104 (w), 1340 (m), 1439 (m), 1459 (m), 1614 (m), 2919 (s), 3094 (s), 3391 (s). Anal. Calc. For $C_{22}H_{18}N_{10}P_2F_{12}Ru$: C, 32.5; H, 2.2; N, 17.2. Found: C, 33.0; H, 2.6; N, 16.9%. ESI-MS: m/z 262 $\{M - 2(PF_6)\}^{2+}$, 523 $\{M - (PF_6) - H\}^+$. ^1H NMR (250 MHz, CD_3OD): δ (ppm) 8.32–8.24 (6H, m, pyridine $H^{3/5}$ and H^4), 7.59 (4H, d, J = 2.8; pyrazolyl H^5), 7.21 (4H, d, J = 2.8 Hz; pyrazolyl H^4). UV/Vis in MeCN: λ_{max}/nm ($10^{-3}\varepsilon/M^{-1}$ cm^{-1}) 418 (16.4), 302 (33.1), 290 (33.1), 232 (39.0).

The second (minor) red band was evaporated to dryness *in vacuo* and the residue was dissolved in MeCN–EtOH (10 cm^3, 1 : 1 v/v), which was filtered to remove KNO_3. Diffusion of diethyl ether into the concentrated red filtrate gave $[Ru(H_2bpp)_2][NO_3]_2$ as red crystals. Yield: 20%. IR (KBr pellet, cm^{-1}): ν (cm^{-1}) 1384 (s, NO_3^-). ESI-MS: m/z 262 $\{M - 2(NO_3^-)\}^{2+}$. This could be simply converted to the hexafluorophosphate salt by dissolving it in water and adding NH_4PF_6 to precipitate it.

$[Ru(L^1)_2](PF_6)_2$. A mixture of $[Ru(H_2bpp)_2][PF_6]_2$ (0.204 g, 0.25 mmol), 2-[1-{4-(bromomethyl)benzyl}-1*H*-pyrazol-3-yl]-pyridine (0.410 g, 1.25 mmol), Bu_4NI (0.046 g, 0.125 mmol), MeCN (60 cm^3) and CH_2Cl_2 (20 cm^3) was stirred at 80 °C for 10 min. Then a solution of NaH (60% dispersion in mineral oil; 0.060 g, 2.50 mmol) in MeCN (20 cm^3) was added dropwise, and the dark red suspension was stirred at 80 °C for 50 h. After cooling, the red mixture was then filtered to remove any solids, and the filtrate was evaporated *in vacuo*. The red residue was dissolved in 2 cm^3 of acetonitrile which was loaded onto a silica gel column. The main orange–red band was collected by elution with acetonitrile–water–saturated aqueous KNO_3 (40 : 4 : 1) as eluent, and reduced in volume until the organic part of the solvent mixture was removed; the complexes were precipitated from the residual aqueous solution by addition of aqueous NH_4PF_6, and filtered off. To ensure complete removal of traces of KNO_3 and NH_4PF_6, the solid was dissolved in acetonitrile, an equal volume of water added, and the mixture concentrated *in vacuo* until the complex reprecipitated and was again filtered off, washed well with water, and dried. The orange solid was dissolved in MeCN–EtOH (5 : 1 v/v) and left to evaporate slowly in air for a few days to gave orange–red crystals of $[Ru(L^1)_2](PF_6)_2$. Yield: 26%. Anal. Calc. For $C_{86}H_{70}N_{22}P_2F_{12}Ru \cdot MeCN$: C, 57.3; H, 4.0; N, 17.5. Found: C, 57.8; H, 3.8; N, 17.8%. Main IR peaks (KBr pellet, cm^{-1}): ν 557 (m), 769 (m) 845 (s, PF_6^-), 1229 (w),

1349 (m), 1384 (m), 1451 (m), 1594 (w), 1615 (w), 2927 (w), 3135 (w), 3418 (s). ESI-MS: m/z 756 $\{M - 2(PF_6)\}^{2+}$. ^{1}H NMR (500 MHz, CD_3CN): δ (ppm) 8.53 (4H, d, J = 4.2; pyridyl H^6), 7.96–7.90 (6H, m; 4 × pyridyl H^3 and 2 × coordinated pyridyl H^4), 7.73–7.76 (8H, m; 4 × pyridyl H^4, 4 × pyrazolyl H), 7.58 (4H, d, J = 7.9; coordinated pyridyl H^3), 7.23 (4H, ddd, J = 1.1, 4.8, 7.5; pendant pyridyl H^5), 7.21 (4H, d, J = 2.8; pyrazolyl H), 6.93 (d, 4H, J = 2.4; pyrazolyl H), 6.83 (8H, d, J = 8.3; phenyl), 6.34 (4H, d, J = 2.9; pyrazolyl H), 5.75 (8H, d, J = 8.2 Hz, phenyl), 5.22 (8H, s; CH_2), 4.18 (8H, s; CH_2). UV/Vis in MeCN: λ_{max}/nm ($10^{-3}\varepsilon$/M^{-1} cm^{-1}) 402 (16.4), 316 (41.4), 274 (68.4), 252 (90.8).

$[Ru(L^2)_2][PF_6]_2$. A mixture of $[Ru(H_2bpp)_2][PF_6]_2$ (0.504 g, 0.62 mmol), 4′-[(4-bromomethyl)phenyl]terpyridine (1.250 g, 3.11 mmol), Bu_4NI (0.115 g, 0.311 mmol), MeCN (150 cm^3) and CH_2Cl_2 (70 cm^3) was stirred at 85 °C for 10 min. Then a solution of NaH (60% dispersion in mineral oil; 0.149 g, 6.21 mmol) in MeCN (60 cm^3) was added dropwise, and the dark red suspension was stirred at 85 °C for 50 h. After cooling, the red mixture was then filtered to remove any solids, and the filtrate was evaporated *in vacuo*. The red residue was washed with water (3 × 100 cm^3) and benzene (3 × 100 cm^3). After drying, the red residue was recrystallized from dmf/diethyl ether to give red crystals of $[Ru(L^2)_2][PF_6]_2$. Yield: 49%. Anal. Calc. For $C_{110}H_{78}N_{22}P_2F_{12}Ru \cdot C_6H_6$: C, 64.0; H, 3.9; N, 14.2. Found: C, 63.4; H, 3.9; N, 13.9%. ESI-MS: m/z 904.3 $\{M - 2(PF_6)\}^{2+}$. ^{1}H NMR (500 MHz, CD_3CN): δ (ppm) 8.64 (8H, s; pendant pyridyl $H^{3'/5'}$), 8.62–8.59 (16H, m; 8 × pendant pyridyl $H^{6/6''}$ and 8 × pendant pyridyl $H^{3/3''}$), 8.25 (2H, t, J = 8.1; coordinated pyridyl H^4), 7.97 (4H, d, J = 7.9; coordinated pyridyl $H^{3/5}$), 7.92 (8H, ddd, J = 1.1, 4.8, 7.5; pendant pyridyl $H^{5/5''}$), 7.59 (4H, d, J = 2.9; pyrazolyl H), 7.54 (8H, d, J = 8.5; phenyl), 7.37–7.34 (8H, m; pendant pyridyl $H^{4/4''}$), 6.76 (4H, d, J = 2.8; pyrazolyl H), 6.19 (8H, d, J = 8.4 Hz; phenyl), 4.52 (8H, s; CH_2). UV/Vis in CH_2Cl_2: λ_{max}/nm ($10^{-3}\varepsilon$/M^{-1} cm^{-1}) 402 (17.2), 316 (79.9), 276 (163), 254 (164), 230 (113). Main IR peaks (KBr pellet, cm^{-1}): ν 557 (m), 793 (m), 845 (s, PF_6^-), 108 (m), 1122 (m), 1246 (w), 1384 (s), 1451 (m), 1468 (m), 1585 (m), 1616 (m), 3448 (s).

$[RuAg_2(L^1)_2][ClO_4]_4$. $AgClO_4 \cdot H_2O$ (125 mg, 0.55 mmol) was added to a stirred solution of $[Ru(L^1)_2](PF_6)_2$ (180 mg, 0.10 mmol) in freshly distilled MeCN (8 cm^3) at room temperature and stirred in the dark for 24 h to afford a red suspension. The solvent was removed and the red residue was dissolved in hot dmf (5 cm^3). Diffusion of diethyl ether–diisopropyl ether (1 : 1) into the dmf solution gave the product $[RuAg_2(L^1)_2][ClO_4]_4$ as red crystals. Yield: 86%. Anal. Calc. For $C_{86}H_{70}N_{22}Cl_4O_{16}RuAg_2 \cdot 2H_2O$: C, 47.8; H, 3.4; N, 14.3. Found: C, 47.3; H, 3.9; N, 14.6%. ESI-MS: m/z 405.5 $\{M - Ag - 4(ClO_4)\}^{4+}$, 432 $\{M - 4(ClO_4)\}^{4+}$, 540 $\{M - Ag - 4(ClO_4)\}^{3+}$, 609 $\{M - 3(ClO_4)\}^{3+}$, 860 $\{M - Ag - 3(ClO_4)\}^{2+}$, 964 $\{M - 2(ClO_4)\}^{2+}$. ^{1}H NMR [500 MHz, $(CD_3)_2SO$]: δ (ppm) 8.67 (4H, d, J = 5.0; pyridyl H^6), 8.29 (2H, t, J = 8.1; central pyridyl H^4), 8.20 (4H, d, J = 7.9; central pyridyl $H^{3/5}$), 8.15 (4H, d, J = 2.2; pyrazolyl H), 7.98–7.94 (8H, m; 4 × pyridyl H^3, 4 × pyridyl H^4), 7.48 (4H, m; pyridyl H^5), 7.31 (4H, d, J = 2.2; pyrazolyl H), 7.10 (4H, d, J = 2.2; pyrazolyl H), 6.95 (4H, d, J = 2.2; pyrazolyl H), 6.47 (8H, d, J = 8.1; phenyl), 5.64 (8H, d, J = 8.1 Hz; phenyl), 5.07 (8H, br s; CH_2 4.04 (8H, br s; CH_2). UV/Vis in dmf: λ_{max}/nm ($10^{-3}\varepsilon$/M^{-1} cm^{-1}) 404 (20.6), 302 (57.2), 272 (89.6). Main IR peaks (KBr pellet, cm^{-1}): ν 624 (m), 770 (m), 1108 (s), 1121 (s), 1235 (w), 1385 (m), 1433 (m), 1452 (m), 1664 (s), 3135 (m), 3422 (s).

$[RuCu_4(MeCN)_5(H_2O)_{1.5}(L^2)_2](SbF_6)_6(BF_4)_4 \cdot 5H_2O$. A solution of $Cu(BF_4)_2$ hydrate (0.400 g, 1.69 mmol) in methanol (7 cm^3) was added dropwise to a stirred red solution of $[Ru(L^2)_2][PF_6]_2$ (0.210 g, 0.1 mmol) in $MeCN/CH_2Cl_2$ (1 : 1 v/v, 20 cm^3) at room temperature to give a clear brown-green solution which was stirred for 1 day. A solution of excess (10 equiv.) $NaSbF_6$ in MeCN was then added and the solution stirred for another 1 h. The mixture was evaporated to dryness *in vacuo*; the residue was dissolved in nitromethane (15 cm^3) and then was filtered to remove any solids. Slow diffusion of diethyl ether–diisopropyl ether (1 : 1) into the concentrated nitromethane solution gave the pentanuclear product as brown–green crystals. Yield: 25%. Anal. Calc. For $C_{110}H_{78}N_{22}F_{56}B_2Cu_4RuSb_8$: C, 32.1; H, 1.9; N, 7.5. Found: C, 31.8; H, 2.1; N, 7.2%. ESI-MS: m/z 652.5 $\{RuCu_4(H_2O)(L^2)_2(SbF_6)_5\}^{5+}$. Main IR peaks (KBr pellet, cm^{-1}): ν 660 (s, SbF_6^-), 792 (m), 1084 (s, BF_4^-) 1250 (w), 1384 (w), 1478 (w), 1609 (m), 1659 (m), 1707 (m), 2925 (w), 3438 (s). UV/Vis in MeCN: λ_{max}/nm (10^{-3} ε/M^{-1} cm^{-1}) 400 (18.9), 315 (117), 290 (148), 270 (111).

X-Ray crystallography

X-ray crystallographic data are summarised in Table 6. In each case a suitable crystal was coated with hydrocarbon oil and attached to the tip of a glass fibre and transferred to a Bruker APEX-2 CCD diffractometer (graphite monochromated Mo-Kα radiation, λ = 0.71073 Å) under a stream of cold N_2. After collection and integration the data were corrected for Lorentz and polarisation effects and for absorption by semi-empirical methods (SADABS)[18] based on symmetry-equivalent and repeated reflections. The structures were solved by direct methods or heavy atom Patterson methods and refined by full matrix least squares methods on F^2. Hydrogen atoms were placed geometrically and refined with a riding model and with U_{iso} constrained to be 1.2 (1.5 for methyl groups) times U_{eq} of the carrier atom. Structures were solved and refined using the SHELX suite of programs.[19] Significant bond distances and angles for the structures of the metal complexes are in Tables 1–5. Particular problems associated with the refinements are as follows.

$[Ru(H_2bpp)_2][PF_6]_2 \cdot 2Et_2O \cdot 2MeCN$. One of the hexafluorophosphate anions exhibits disorder with four of the F atoms [F(9), F(10), F(11) and F(12)] disordered over two sites (occupancies 0.59/0.41). One of the $CH_3CH_2OCH_2CH_3$ molecules was disordered with the four carbon atoms [C(02)–C(05)] split over two sites (site occupancies 0.54/0.46); likewise the terminal methyl group of one MeCN molecule [atom C(110)] was disordered over two sites with occupancies of 0.48/0.52. All disordered atoms were refined with isotropic thermal displacement parameters.

Table 6 Summary of crystal data, data collection and refinement parameters for the new structures

Complex	$[Ru(H_2bpp)_2][PF_6]_2 \cdot 2Et_2O \cdot 2MeCN$	$[Ru(L^1)_2](NO_3)_2 \cdot 4H_2O$	$[Ru(L^2)_2][PF_6]_2 \cdot C_6H_6$	$[RuAg_2(L^1)_2][ClO_4]_4 \cdot H_2O \cdot 2dmf$	$[RuCu_4(MeCN)_5(H_2O)_{1.5}(L^2)_2](SbF_6)_6(BF_4)_4 \cdot 5H_2O$
Formula	$C_{34}H_{44}F_{12}N_{12}O_2P_2Ru$	$C_{86}H_{78}N_{24}O_{10}Ru$	$C_{116}H_{84}F_{12}N_{22}P_2Ru$	$C_{92}H_{84}Ag_2Cl_4N_{24}O_{19}Ru$	$C_{120}H_{107}B_4Cu_4F_{52}N_{26}O_{6.5}Ru\ Sb_6$
M	1043.82	1708.79	2177.06	2288.44	4134.29
T/K	150(2)	150(2)	100(2)	100(2)	150(2)
Crystal system	Monoclinic	Tetragonal	Orthorhombic	Monoclinic	Monoclinic
Space group	$C2/c$	$I\bar{4}$	$Pnna$	$C2/c$	$P2_1/c$
a/Å	25.6147(16)	16.7252(5)	27.3364(11)	30.736(4)	16.1145(8)
b/Å	10.1935(6)	16.7252(5)	15.9057(6)	14.284(2)	43.921(2)
c/Å	36.361(2)	16.1385(10)	24.5589(9)	21.992(3)	24.9915(12)
β/°	105.085(4)	90	90	98.756(9)	96.158(3)
V/Å^3	9166.8(10)	4514.5(3)	10 678.3(7)	9543(2)	17 586.1(15)
Z	8	2	4	4	4
D_c/Mg m^{-3}	1.513	1.257	1.354	1.593	1.561
μ/mm^{-1}	0.506	0.242	0.258	0.757	1.568
Reflections collected	53 604	62 954	175 242	64 337	127 534
Independent reflections	10 549	8235	9418	8394	23 020
R_{int}	0.0827	0.0315	0.0560	0.0759	0.0517
Data/restraints/parameters	10 549/17/565	8235/0/249	9418/4/723	8394/32/642	23 020/311/1904
Final $R1$, $wR2$ indices[a]	0.0553, 0.1475	0.0582, 0.1532	0.0599, 0.1837	0.0675, 0.1943	0.1281, 0.3847

[a] $R1 = \sum||F_o| - |F_c||/\sum|F_o|$ for 'observed data'; $wR2 = [\sum w(F_o^2 - F_c^2)^2/\sum w(F_o^2)^2]^{1/2}$ for all unique data.

$[Ru(L^1)_2](NO_3)_2 \cdot 4H_2O$. The Ru atom lies on a $\bar{4}$ symmetry axis; thus only one quarter of the molecule (*i.e.* half of a ligand) lies in the asymmetric unit, which also contains two water molecules in general positions (site occupancy 0.5 for each). The nitrate anions could not be located, presumably due to extensive disorder, and are absent from the refinement; a large number of small residual electron density peaks was apparent. Application of the SQUEEZE function in PLATON was used to remove these. Note that the pendant pyrazolyl–pyridine ring has the N atoms N(11) and N(21) *syn* to one another, rather than the more usual *anti* conformation which might be expected if these N atoms were to avoid each other. This is because both of these N atoms are involved in a hydrogen-bonding interaction with a nearby water molecule in an adjacent asymmetric unit [O(100)], with non-bonded distances N(11)···O(100A) and N(21)···O(100A) of 3.12 and 3.10 Å, respectively. Although the H atoms were not located for this water molecule, it is reasonable to assume a chelating H-bonding interaction in which both N(11) and N(21) interact with the same proton.

$[Ru(L^2)_2][PF_6]_2 \cdot C_6H_6$. The complex cation lies on a twofold axis such that the asymmetric unit contains half of a Ru atom and one unique ligand L^2. One hexafluorophosphate anion [containing P(1)] is in a general position with all atoms having a site occupancy of 0.5; the other lies on a twofold symmetry element such that half of it lies in the asymmetric unit. The SQUEEZE function in PLATON was applied to eliminate diffuse areas of residual electron density that presumably arise from disordered lattice solvent but could not be satisfactorily modeled.

$[RuAg_2(L^1)_2][ClO_4]_4 \cdot H_2O \cdot 2dmf$. The complex cation lies on a twofold symmetry element which passes through the Ru atom, such that the asymmetric unit contains 0.5 of the Ru atom and one Ag atom. The lattice water molecule is in a general position (hydrogen-bonded to the two independent perchlorate anions) but refines satisfactorily with a site occupancy of 0.5. This structural determination presented no significant problems.

$[RuCu_4(MeCN)_5(H_2O)_{1.5}(L^2)_2](SbF_6)_6(BF_4)_4 \cdot 5H_2O$. There is no imposed symmetry, with an entire independent formula unit in the asymmetric unit. There is extensive disorder of the tetrafluoroborate/hexafluoroantimonate anions; these needed to be refined with partial site occupancies for disordered F atoms, and extensive use of geometric restraints to keep the geometries approximately reasonable. Many of the disordered atoms needed to be refined with isotropic displacement parameters to keep the refinement stable. Application of the SQUEEZE function in PLATON was used to remove areas of severe disorder (probably of lattice solvent) which could not be satisfactorily modeled. For these reasons the final $R1$ value is relatively poor (12.8%) although the structure of the complex cation is perfectly clearly defined.

CCDC reference numbers 659047–659051.

For crystallographic data in CIF or other electronic format see DOI: 10.1039/b708572a

Acknowledgements

We thank the Royal Society for a post-doctoral fellowship to Q.-H. W.

References

1 (*a*) A. Jansco, S. Mikkola, H. Lonnberg, K. Hegetschweiler and T. Gajda, *Chem.–Eur. J.*, 2003, **9**, 5404; (*b*) H. Ohtsu, Y. Shimazaki, A. Odani, O. Yamauchi, W. Mori, S. Itoh and S. Fukuzumi, *J. Am. Chem. Soc.*, 2000, **122**, 5733; (*c*) B. M. Trost and S. Hisaindee, *Org. Lett.*, 2006, **8**, 6003; (*d*) M. Lanznaster, A. Neves, A. J. Bortoluzzi, B. Szpoganicz and E. Schwingel, *Inorg. Chem.*, 2002, **41**, 5641.

2 (*a*) S. Goeb, A. De Nicola, R. Ziessel, C. Sabatini, A. Barbieri and F. Barigelletti, *Inorg. Chem.*, 2006, **45**, 1173; (*b*) T. Lazarides, T. L. Easun, C. Veyne-Marti, W. Z. Alsindi, M. W. George,

N. Deppermann, C. A. Hunter, H. Adams, G. M. Davies and M. D. Ward, *J. Am. Chem. Soc*., 2007, **129**, 4014; (*c*) K. Senechal-David, S. J. A. Pope, S. Quinn, S. Faulkner and T. Gunnlaugsson, *Inorg. Chem*., 2006, **45**, 10040; (*d*) S. Encinas, L. Flamigni, F. Barigelletti, E. C. Constable, C. E. Housecroft, E. R. Schofield, E. Figgemeier, D. Fenske, M. Neuburger, J. G. Vos and M. Zehnder, *Chem.–Eur. J*., 2002, **8**, 137.

3 D. M. D'Alessandro, M. S. Davies and F. R. Keene, *Inorg. Chem*., 2006, **45**, 1656.

4 S. P. Argent, H. Adams, L. P. Harding, T. Riis-Johannessen, J. C. Jeffery and M. D. Ward, *New J. Chem*., 2005, **29**, 904.

5 M. Sommovigo, G. Denti, S. Serroni, S. Campagna, C. Mingazzini, C. Mariotti and A. Juris, *Inorg. Chem*., 2001, **40**, 3318.

6 (*a*) E. C. Constable, C. E. Housecroft and I. Poleschak, *Inorg. Chem. Commun*., 1999, **2**, 565; (*b*) E. C. Constable, C. E. Housecroft, M. Neuburger, S. Schaffner and L. J. Scherer, *Dalton Trans*., 2004, 2635; (*c*) E. C. Constable, R. W. Handel, C. E. Housecroft, A. F. Morales, B. Ventura, L. Flamigni and F. Barigelletti, *Chem.–Eur. J*., 2005, **11**, 4024; (*d*) E. C. Constable, A. M. W. Cargill Thompson, P. Harveson, L. Macko and M. Zehnder, *Chem.–Eur. J*., 1995, 360.

7 (*a*) Y. Tor, *Synlett*, 2002, 1043; (*b*) P. J. Connors, D. Tzalis, A. L. Dunnick and Y. Z. Tor, *Inorg. Chem*., 1998, **37**, 1121; (*c*) D. Tzalis and Y. Tor, *Angew. Chem., Int. Ed. Engl*., 1997, **36**, 2666.

8 D. A. Bardwell, J. C. Jeffery, P. L. Jones, J. A. McCleverty, E. Psillakis, Z. Reeves and M. D. Ward, *J. Chem. Soc., Dalton Trans*., 1997, 2079.

9 E. C. Constable, *Adv. Inorg. Chem. Radiochem*., 1986, **30**, 69.

10 D. L. Jameson, J. K. Blaho, K. T. Kruger and K. A. Goldsby, *Inorg. Chem*., 1989, **28**, 4312, and references therein.

11 A. Juris, V. Balzani, F. Barigeletti, S. Campagna, P. Belser and A. von Zelewsky, *Coord. Chem. Rev*., 1988, **84**, 85.

12 A. B. P. Lever, *Inorg. Chem*., 1990, **29**, 1271.

13 (*a*) C. O. Dietrich-Buchecker, P. A. Marnot, J.-P. Sauvage, J.-P. Kintinger and P. Maltese, *New J. Chem*., 1984, **8**, 573; (*b*) J. R. Kirchhoff, D. R. McMillin, P. A. Marnot and J.-P. Sauvage, *J. Am. Chem. Soc*., 1985, **107**, 1138.

14 J. P. Sauvage and M. Ward, *Inorg. Chem*., 1991, **30**, 3869.

15 (*a*) S. P. Argent, H. Adams, T. Riis-Johannessen, J. C. Jeffery, L. P. Harding, W. Clegg, R. W. Harrington and M. D. Ward, *Dalton Trans*., 2006, 4996; (*b*) C. Piguet, G. Bernardinelli, A. F. Williams and B. Bocquet, *Angew. Chem., Int. Ed. Engl*., 1995, **34**, 582.

16 (*a*) P. K. K. Ho, K. K. Cheung and C.-M. Che, *Chem. Commun*., 1996, 1197; (*b*) A. C. G. Hotze, B. M. Kariuki and M. J. Hannon, *Angew. Chem., Int. Ed*., 2006, **45**, 4839; (*c*) S. L. Larson, S. M. Hendrickson, S. Ferrere, D. L. Derr and C. M. Elliott, *J. Am. Chem. Soc*., 1995, **117**, 5881; (*d*) J. D. Crane and J.-P. Sauvage, *New J. Chem*., 1992, **16**, 649; (*e*) M. H. W. Lam, S. T. C. Cheung, K.-M. Fung and W.-T. Wong, *Inorg. Chem*., 1997, **36**, 4618; (*f*) N. C. Fletcher, R. T. Brown and A. P. Doherty, *Inorg. Chem*., 2006, **45**, 6132; (*g*) S. Torelli, S. Delahaye, A. Hauser, G. Bernardinelli and C. Piguet, *Chem.–Eur. J*., 2004, **10**, 3503; (*h*) G. I. Pascu, A. C. G. Hotze, C. Sanchez Cano, M. M. Kariuki and M. J. Hannon, *Angew. Chem., Int. Ed*., 2007, **46**, 4374.

17 (*a*) J.-P. Collin, S. Guillerez, J.-P. Sauvage, F. Barigelletti, L. De Cola, L. Flamigni and V. Balzani, *Inorg. Chem*., 1991, **30**, 4230; (*b*) W. Spahni and G. Calzaferri, *Helv. Chim. Acta*, 1984, **67**, 450.

18 G. M. Sheldrick, *SADABS version 2.10*, University of Göttingen, 2003.

19 G. M. Sheldrick, *SHELXS-97 and SHELXL-97*, University of Göttingen, 1997.

